



Isothermal (Vapour + Liquid) Equilibrium Measurements and Correlation of the Binary Mixture {3,3,3-Trifluoropropene (HFO-1243zf) + 2,3,3,3-tetrafluoropropene (HFO-1234yf)} at Temperatures from 283.15 K to 323.15 K

L. Fedele¹ · G. Lombardo^{1,2} · D. Menegazzo^{1,2} · M. Scattolini¹ · S. Bobbo¹

Received: 27 December 2022 / Accepted: 16 March 2023

© The Author(s) 2023

Abstract

The many constraints introduced by the F-gas Regulation and the Kigali Amendment to the Montreal Protocol have resulted in an intense search for alternatives to fluorinated greenhouse gases for air conditioning and refrigeration purposes (Mota-Babiloni A, Makhnatch P, in *Int J Refrig* 127:101–110, 2021). With respect to the urge of new low-GWP and low-ODP refrigerants, blends composed of hydrofluoroolefins (HFO) are considered promising possible substitutes to hydrofluorocarbons (HFCs) and hydrochlorofluorocarbons (HCFCs) for HVAC&R applications (Sovacool et al., in *Renew Sustain Energy Rev* 141:110759), but thermophysical properties data for these blends are still scarce (Bell et al., in: *J Chem Eng Data*, 2021). In the present study, the vapor–liquid equilibrium (VLE) for the binary system (HFO-1243zf + HFO-1234yf), for which just one set of data on the VLE is available to date in literature, has been experimentally studied by means of a vapor recirculation apparatus. The measurements have been performed at isothermal conditions in the range of temperatures between 283.15 K and 323.15 K, while the composition of both the phases in equilibrium has been measured by gas-chromatographic analysis. The experimental VLE data have been correlated by two different equations of state (EoS): the Peng–Robinson (PR) EoS combined with Mathias–Copeman (MC) alpha function and van der Waals (vdW) mixing rules, and the Helmholtz EoS with dedicated binary interaction parameters. Correlated results showed a good agreement with the experimental data for the binary system.

Keywords Low GWP · Hydrofluoroolefins · Heat pump · VLE

Selected Papers of the 13th Asian Thermophysical Properties Conference.

✉ L. Fedele
fedele@itc.cnr.it

Extended author information available on the last page of the article

Published online: 17 April 2023

1 Introduction

In the air conditioning and refrigeration industry (HVAC&R), the replacement of existing refrigerants with fluids with a lower environmental impact plays an increasingly central role [1]. The Kigali Amendment to the Montreal Protocol in 2016 [2] and even earlier, at European level, the EU Regulation No 517/2014 (better known as F-gas Regulation [3]), called for a progressive phase down in the production and consumption of HFC-based refrigerants, considered potent contributors to climate change due to their severe global warming potential (GWP). For instance, R134a and R410A, which represent the dominate refrigerants for air conditioning and refrigeration applications (both domestic and commercial), present a GWP of 1530 and 2256 respectively [4], definitely higher than the 150 GWP limit prescribed by the F-gas Regulation [3] on the long term. In the pursuit for low-GWP and low-ODP refrigerants a number of constraints, including thermophysical and thermodynamic properties, safety, chemical stability and compatibility with materials, and last but not least availability and cost, narrows the number of potential fluids [5]. In this perspective, blends composed of hydro-fluoroolefins (HFO) have raised attention as the most promising alternatives to HFCs for HVAC&R applications [6], since they present similar thermodynamic properties, together with an ODP equal to zero and extremely low GWPs, but thermophysical properties data for these blends are still scarce [7]. Among HFOs, 2,3,3,3-tetrafluoropropene (R1234yf) and 3,3,3-trifluoropropene (R1243zf), represent potential alternatives in refrigeration and heat pump systems, with ODP = 0 and GWP < 1 [4], and their performances as pure fluids have been compared to that of R134a in previous research [8–10].

In particular, R1234yf is by far the most investigated HFO, and a wide literature analysis regarding its thermophysical properties has been performed by Bobbo et al. [5], newly updated by Fedele et al. [11]. On the other hand, R1243zf has recently gained interest, having similar thermophysical properties of R134a and a lower price than R1234yf [12]; a number of studies has now been gathered about its thermodynamic properties, including critical point [13], vapour pressure [12, 14–17], $p\nu T$ properties [13, 16, 18], specific heat capacity [19, 20] and speed of sound [21]. Analogously, also the transport properties of R1243zf, i.e. thermal conductivity [22], viscosity and surface tension [23, 24], have been researched more extensively. However, the flammability of R1234yf and R1243zf, classified as mildly flammable (A2L) and flammable (A2), respectively, and their reduced refrigerating capacity compared to HFCs increase their potential when used in blends [9]. Nowadays, several multi-component mixtures including either R1234yf or R1243zf have been presented as alternatives for the next-generation refrigerants [5, 8, 9, 12, 15, 25, 26]; nevertheless, to date only one study has been published on the thermodynamic properties of the binary mixture R1234yf + R1243zf [27], and accurate vapour-liquid equilibrium measurements of the blend, which are essential for the evaluation of its performance potential in a refrigeration cycle and the designing of the eventual refrigeration system, are still scarce. To compensate for this lack of information in the present study

the isothermal vapor–liquid equilibrium (VLE) for the binary system (HFO-1243zf + HFO-1234yf) was experimentally studied by means of a vapor recirculation apparatus at five temperatures in the range between 283.15 K and 323.15 K. The experimental VLE data were then compared with available literature and correlated by two different equations of state (EoS): the Peng–Robinson (PR) EoS combined with Mathias–Copeman (MC) alpha function and van der Waals (vdW) mixing rules and the Helmholtz EoS with dedicated binary interaction parameters. Finally, a further comparison was made with data correlated using the Helmholtz EoS currently implemented in REFPROP 10.0.

2 Experimental

2.1 Materials

Table 1 summarizes the information on the R1234yf and R1243zf samples used in this study. In order to remove the non-condensable gases, the samples underwent several freeze–pump–thaw cycles with liquid nitrogen. Their purity was then verified by gas-chromatography analysis using a thermal conductivity detector (TCD). The samples were then used without further purification.

2.2 Apparatus

The experimental setup used in this study was thoroughly described in previous work [28], thus only its salient features are presented here. The vapor recirculation apparatus consists of a visual VLE cell equipped with a magnetic pump, both immersed in a thermostatic water bath of about 100 l capacity. Inside the VLE cell, made of stainless steel and with an internal volume of 50 cm³, a faster thermodynamic equilibrium is reached thanks to the action of a magnetic pump, that ensures an intensive circulation of the vapor phase into the liquid one. The temperature inside the bath is stabilized by means of a PID-controlled system that operates on a heater immersed in the bath, while an auxiliary thermostatic bath is used to compensate for the heat produced by the PID-controlled system and to reach the desired level of temperature in the main bath. Temperature is measured with a 100Ω platinum resistance thermometer and continuously recorded by means of a multimeter (Hewlett-Packard 3458). Temperature stability in the bath is ± 1 mK, and its expanded uncertainty (k = 1) was assessed to be ± 0.02 K.

Table 1 Chemical information on the samples

Substance	Structural formula	Supplier	Purity (mass fraction) ^a
R1234yf	CH ₂ =CF–CF ₃	Chemours	0.998
R1243zf	CH ₂ =CH–CF ₃	Mexichem	0.999

^aGC analysis

Pressure is measured by means of a pressure gauge (Ruska 6000) with a full scale of 17,000 kPa and an expanded uncertainty ($k=1$) of ± 1 kPa, considering both the accuracy of the pressure transducer and the stability of the pressure during the measurements. The compositions of the phases are then analyzed by a gas chromatograph (Hewlett-Packard 6890) connected on-line to the VLE cell and equipped with a TCD detector, previously calibrated by means of gravimetrically-prepared mixtures. As explained in [28], the expanded uncertainty ($k=2$) in mixture preparation is estimated equal to 0.3 mg, which gave an estimated uncertainty of $0.0001 \text{ mol}\cdot\text{mol}^{-1}$ in molar fraction. The calibration was carried out every day with 8 bottles of different known compositions. For both the calibration and the measurements, the number of repeated measurements on same sample was such that a standard deviation lower than $0.001 \text{ mol}\cdot\text{mol}^{-1}$ was obtained in the molar fraction on three consecutive measurements. Under these assumptions,

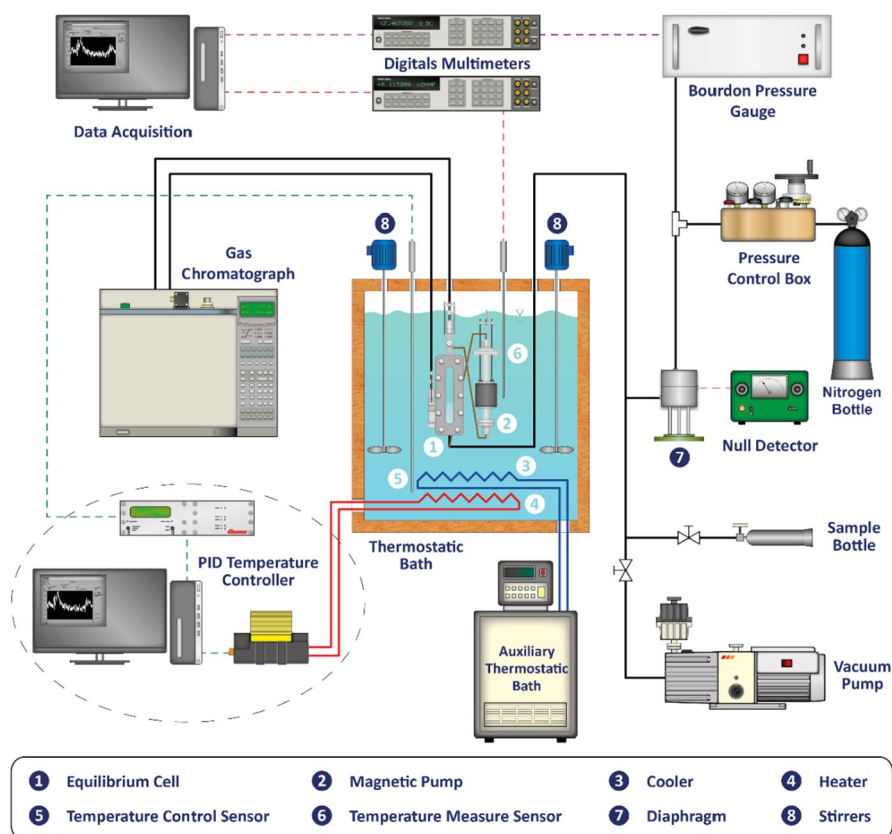


Fig. 1 Schematic of the VLE apparatus. Components: cooler (CR), resistance thermometer for temperature control (CT), diaphragm (DP), equilibrium cell (EC), heating resistor (HR), magnetic pump (MP), resistance thermometer for temperature measurement (MT), nitrogen bottle (NB), pure refrigerant bottle (PB), pressure control pack (PCP), pressure gauge (PG), stirrer (ST), sampling valve (SV), vacuum pump (VP)

the expanded uncertainty ($k=2$) in composition measurements is estimated to be within ± 0.003 in mole fraction. A schematic of the experimental setup is reported in Fig. 1.

3 Results and Discussion

3.1 Vapor pressures of pure compounds

The vapor pressures of pure R1234yf and R1243zf were measured at 5 temperature points from 283.15 K to 323.15 K as shown in Table 2. The data were then compared with calculated results from REFPROP 10.0 [29] and the relative deviations of pressure between measured and calculated values are listed in Table 2, where p_{cal} stands for the calculation data from the Helmholtz EoS implemented in the software [30, 31]. The relative deviations of pressure are graphically displayed in Fig. 2a and b, for R1234yf and R1243zf respectively. Figure 2a and b compare the experimental data from this work with several data reported in literature on the base of the EoS implemented in REFPROP, which thus represents the graphs baselines. Experimental data measured in this work differ from the baseline for about $-0.5\% \div -0.1\%$ for R1243zf and $-0.11\% \div +0.18\%$ for 1234yf. As far as R1243zf is concerned, the major part of literature data is lower than the baseline in all the considered temperature range. In particular, as shown in Fig. 2a, data of Yang et al. [9] agree with our work for temperatures higher than 290 K while for lower temperatures data from Yin et al. [16] are consistent with our measurements. On the other hand, for R1234yf, data presented in this study match well the data of both Tanaka and Higashi [32], Di Nicola et al. [33] and Fedele et al. [34], as displayed in Fig. 2b.

3.2 Experimental Data

Vapour-liquid equilibrium of R1243zf + R1234yf binary system was investigated isothermally at five temperatures, 283.15, 293.15, 303.15, 313.15 and 323.15 K, pressure range from 0.4 MPa to 1,2 MPa. The 41 P–T–x–y experimental data are summarized in Table 3 and plotted in Fig. 3, where x_1 and y_1 indicate the

Table 2 Experimental and calculated vapor pressures of pure compounds

T/K	R1243zf			R1234yf		
	$p_{\text{exp}}/\text{kPa}$	$p_{\text{cal}}/\text{kPa}$	$\delta_p/\%$	$p_{\text{exp}}/\text{kPa}$	$p_{\text{cal}}/\text{kPa}$	$\delta_p/\%$
283.15	374.74	375.36	-0.165	438.15	437.53	0.142
293.15	509.37	509.99	-0.122	592.80	591.72	0.182
303.15	675.02	678.01	-0.443	784.65	783.51	0.145
313.15	880.68	884.28	-0.409	1017.01	1018.40	-0.137
323.15	1130.17	1134.00	-0.339	1300.83	1302.30	-0.113

p_{calc} : REFPROP 10.0 (R1243zf: Akasaka and Lemmon Helmholtz EoS [30]; R1234yf: Richter et al. Helmholtz EoS [31]);
 $\delta p = 100(p_{\text{exp}} - p_{\text{calc}})/p_{\text{exp}}$

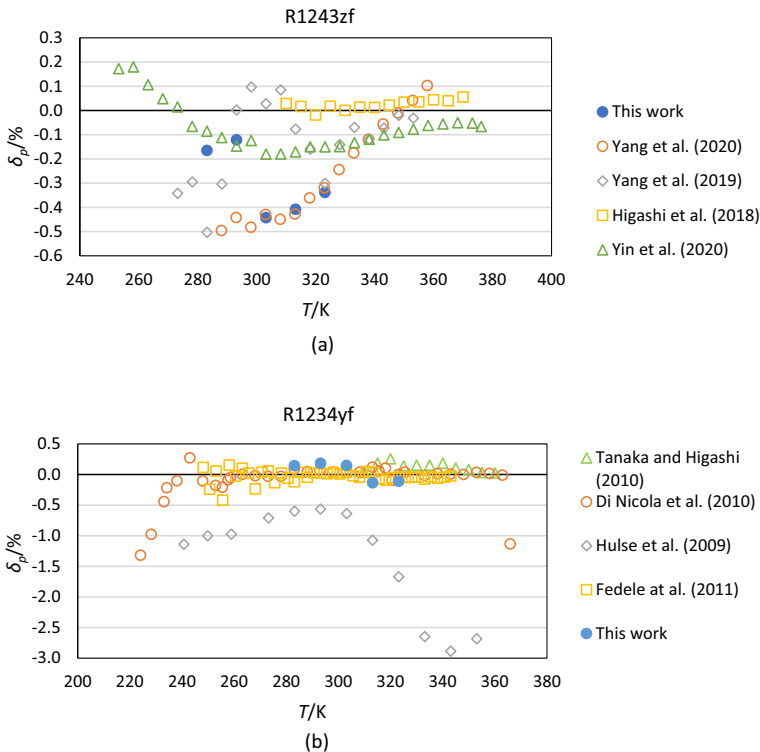


Fig. 2 (a) Relative deviations of vapor pressures compared with the EoS by Akasaka and Lemmon [30] for R1243zf. Literature data: Yang et al. [15], Yang et al. [9], Higashi et al. [14], Yin et al. [16]. (b) Relative deviations of vapor pressure compared with the EoS by Richter et al. [31] for R1234yf. Literature data: Tanaka and Higashi [32], Di Nicola et al. [33], Hulse et al. [35], Fedele et al. [34]

liquid-phase and vapor-phase mole fraction of R1243zf, respectively. As shown in Fig. 3, the binary system demonstrated a near-azeotropic behavior over the entire range of composition.

3.3 Data Reduction

The Peng-Robinson (PR) EoS and the Helmholtz EoS with dedicated binary interaction parameters were applied to model the experimental data. Results were then compared with the Helmholtz EoS implemented in REFPROP 10.0 [29] and literature data by Yang et al. [27].

Peng-Robinson EoS: the PR equation of state is expressed as

$$P = \frac{RT}{v-b} - \frac{a}{v(v+b) + b(v-b)} \quad (1)$$

Table 3 Experimental VLE data for R1243zf (1)+R1234yf (2) at T=283.15, 293.15, 303.15, 313.15, 323.15 K

T=283.15 K			T=293.15 K			T=303.15 K		
x_1	y_1	$p_{\text{exp}}/\text{kPa}$	x_1	y_1	$p_{\text{exp}}/\text{kPa}$	x_1	y_1	$p_{\text{exp}}/\text{kPa}$
0.858	0.8368	384.8	0.8661	0.8475	520.0	0.8779	0.8618	691.5
0.7866	0.7606	389.8	0.7858	0.7614	528.0	0.7909	0.7688	702.2
0.6297	0.5974	401.3	0.666	0.6379	539.0	0.6988	0.6639	713.3
0.5586	0.5254	406.2	0.6144	0.5866	545.5	0.5775	0.5486	726.8
0.4535	0.4224	412.5	0.422	0.395	559.2	0.437	0.4097	741.6
0.3427	0.3168	419.3	0.361	0.3318	564.5	0.358	0.3326	750.2
0.2204	0.2018	425.7	0.2399	0.2217	573.8	0.2399	0.2232	760.2
0.1467	0.1329	430.7	0.12	0.1101	581.9	0.1374	0.124	771.3
			0.0578	0.0513	586.5			
T=313.15 K			T=323.15 K					
x_1	y_1	$p_{\text{exp}}/\text{kPa}$	x_1	y_1	$p_{\text{exp}}/\text{kPa}$			
0.9015	0.8866	897.7	0.8754	0.8614	1156.3			
0.8007	0.7803	913.5	0.8438	0.8273	1161.7			
0.7017	0.6757	928.6	0.788	0.7661	1173.5			
0.5777	0.5494	946.8	0.6882	0.664	1192.3			
0.44	0.4166	961.2	0.5834	0.5578	1210.4			
0.3255	0.2984	976.2	0.488	0.4579	1228.1			
0.1956	0.1804	991.5	0.3838	0.3614	1245.2			
			0.284	0.2625	1261.6			
			0.1449	0.1324	1281.7			

with

$$a_i = 0.45724 \frac{R^2 T_{ci}^2}{P_{ci}} \alpha_i(T) \quad (2)$$

$$b_i = 0.07780 \frac{RT_{ci}}{P_{ci}} \quad (3)$$

where a_i and b_i are, respectively, the energy and the covolume parameter of the i th component; P , T and v are pressure, temperature and molar volume, R is the universal gas constant; T_{ci} and p_{ci} are the critical temperature and critical pressure of the i th component.

In order to obtain a more accurate prediction for pure vapor pressure, for $\alpha_i(T)$ the following alpha function proposed by Mathias and Copeman was followed:

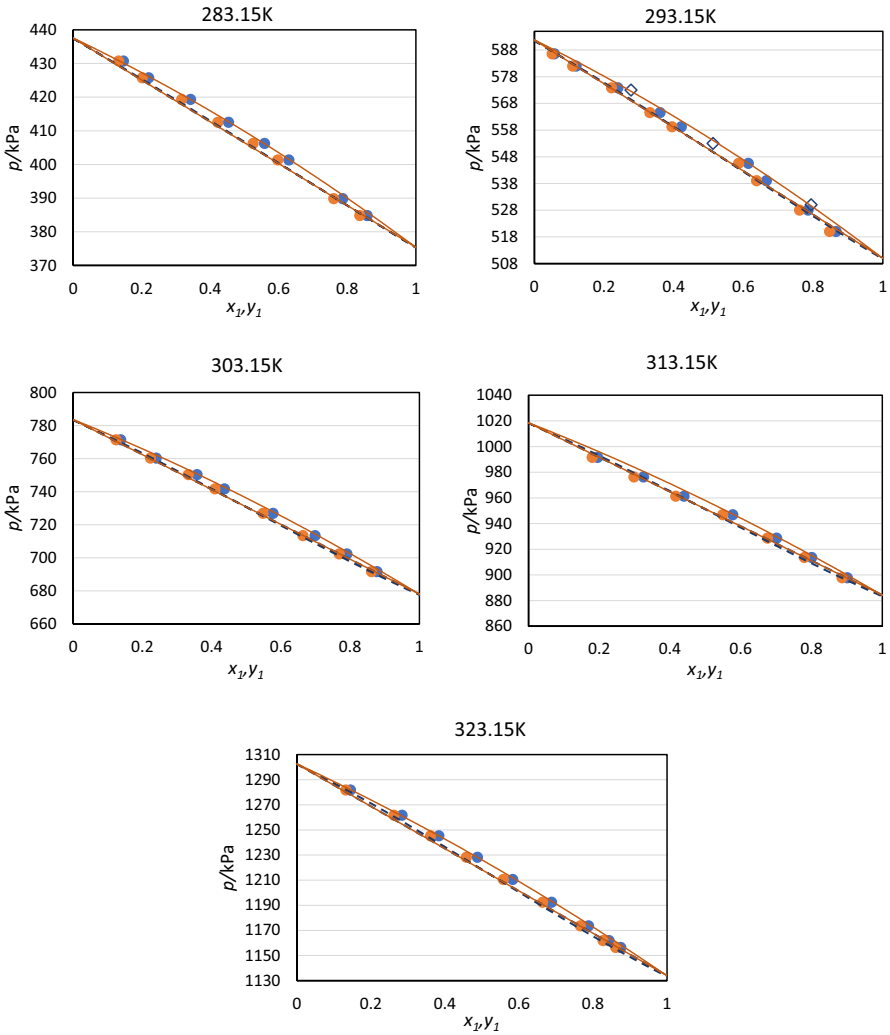


Fig. 3 VLE for the R1243zf (1)+R1234yf (2) binary mixture at 5 different temperatures. Solid points: experimental data; Solid lines: Helmholtz model; dashed lines: PR-MC-VdW model

Table 4 Critical parameters and values of C_1 , C_2 and C_3 of the pure fluids

Fluid	T_c / K	p_c / kPa	C_1	C_2	C_3
R1243zf	376.93	3517.9	0.80529	-0.5758	1.6418
R1234yf	367.85	3382.2	0.8049	-0.4242	1.7469

$$\alpha_i(T) = \left[1 + C_1 \left(1 - \sqrt{\frac{T}{T_{ci}}} \right) + C_2 \left(1 - \sqrt{\frac{T}{T_{ci}}} \right)^2 + C_3 \left(1 - \sqrt{\frac{T}{T_{ci}}} \right)^3 \right]^2 \quad (4)$$

Critical properties of R1234yf and R1243zf T_{ci} and p_{ci} were taken from REPROP 10.0 [29], while for the coefficients C_1, C_2, C_3 of the two pure fluids used in Eq. 4, values taken from the literature were used [9, 36]. The critical properties and the coefficients of MC alpha function are reported in Table 4.

To calculate the energy and the covolume parameters of the EoS for the mixture, a and b respectively, the Van der Waals one-parameter mixing rule was applied:

$$a = \sum_i \sum_j x_i x_j a_{ij} \tag{5}$$

$$a_{ij} = (1 - k_{ij}) \sqrt{a_i a_j} \tag{6}$$

$$b = \sum_i x_i b_i \tag{7}$$

where x_i is the mole fraction of the i th component and k_{ij} is the binary interaction parameter, satisfying the condition $k_{ij} = k_{ji}$ and $k_{ii} = k_{jj} = 0$. The binary interaction parameter was regressed to the experimental data by minimizing the objective function:

$$F_{obj} = \sqrt{\frac{1}{N} \sum_i (x_{exp,i} - x_{calc,i})^2} + \sqrt{\frac{1}{N} \sum_i (y_{exp,i} - y_{calc,i})^2} \tag{8}$$

where the subscripts exp,i and $calc,i$ are referred to the experimental and calculated liquid, x , and vapour, y , mole fractions of the i -th component. N is the number of experimental data. The regressed value for the binary interaction parameter is shown in Table 5.

Helmoltz EoS: a further EoS was used to model the thermodynamic behavior of the mixture, i.e. the Kunz and Wagner [37] multi-fluid Helmholtz energy model, based on the fact that all the thermodynamic properties can be formulated as function of the Helmholtz energy, such as:

$$p = \rho RT \left(1 + \delta \frac{\partial \alpha^r}{\partial \delta}(\tau, \delta) \right) \tag{9}$$

Table 5 Binary interaction parameters and objective functions of PR-MC-VdW and Helmholtz models

PR-MC-vdW EoS				
k_{12}				OF
0.001122				0.0243
Helmholtz EoS				
β_t	γ_t	β_v	γ_v	OF
0.99981	0.99777	1	1	0.0157

The model is built as function of reduced temperature τ and reduced density δ :

$$\delta = \rho / \rho_{c(\bar{x})} \quad (10)$$

$$\tau = T_{c(\bar{x})} / T \quad (11)$$

$$T_{c,ij} = \beta_{T,ij} \gamma_{T,ij} \frac{x_i + x_j}{\beta_{T,ij}^2 x_i + x_j} (T_{c,i} T_{c,j})^{1/2} \quad (12)$$

$$\frac{1}{\rho_{c,ij}} = \beta_{v,ij} \gamma_{v,ij} \frac{x_i + x_j}{\beta_{v,ij}^2 x_i + x_j} \frac{1}{8} \left(\frac{1}{\rho_{c,i}^{1/3}} + \frac{1}{\rho_{c,j}^{1/3}} \right)^3 \quad (13)$$

where ρ represents the density of the mixture; x_i and x_j are the molar fraction of the i -th and j -th components of the mixture and α^r is the residual part of the dimensionless Helmholtz free energy. Subscripts T and v are referred to temperature and volume for the binary interaction parameters $\beta_{T,ij}$, $\gamma_{T,ij}$, $\beta_{v,ij}$, $\gamma_{v,ij}$, which need to be tuned with experimental data. Since the amount of data was limited and concerned only VLE data, only the parameters $\beta_{T,ij}$ and $\gamma_{T,ij}$ have been fitted [40]. The tuning of the parameters was performed through a heuristic optimization algorithm, Adaptive Search Development Particle Swarm Optimization (ASD-PSO) [38], by minimizing the objective function of Eq. 8. Thermodynamic properties were then computed by REFPROP 10.0 subroutines as bubble and dew point calculations with temperature, vapor and liquid compositions as inputs.

Regressed binary interaction parameters are shown in Table 5. Concerning the fitted parameter for the cubic equation, a first test was made fitting the parameter for each isotherm in order to observe if a dependence on temperature exists. Then, only one parameter has been shown in this work since a standard deviation of $1.4e^{-6}$ was obtained among the parameters for the single isotherms. Thus, the temperature dependence of k_{12} can be considered negligible.

3.4 Discussion

Figure 3 shows the phase diagram of the R1243zf/R1234yf binary system calculated by the PR-MC-VdW and the Helmholtz-type models for each analyzed temperature. On the whole, both the PR-MC-VdW and the Helmholtz models can describe well the experimental data and the near-azeotropic behavior of the mixture, with minor difference between one model and the other.

Figures 4 and 5 show the relative deviations of pressure and the absolute deviations of vapor phase composition calculated by the two models, while numerical values are reported in Table 6. The overall average absolute deviation of pressure (AAD(p)) and the average absolute deviation of vapor phase mole fraction (AAD(y)) are equal to 0.409 % (AAD(p)) and 0.002 m(AAD(y)) with the PR-MC-VdW model and 0.192 % (AAD(p)) and 0.002 (AAD(y)) with the Helmholtz model.

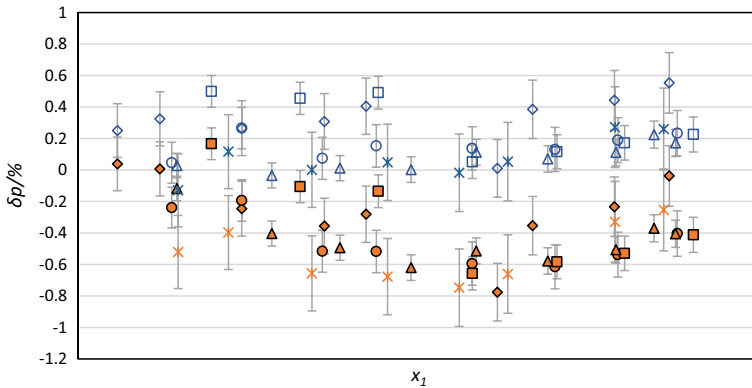


Fig. 4 Relative deviations of pressure for the R1243zf (1)+R1243yf (2) binary mixture from PR-MC-VdW and Helmholtz model. x : 283.15 K (PR-MC-VdW model); x : 283.15 K (Helmholtz model); \diamond : 293.15 K; \circ : 303.15 K; \square : 313.15 K; Δ : 323.15 K. Solid points: PR-MC-VdW model; empty points: Helmholtz model

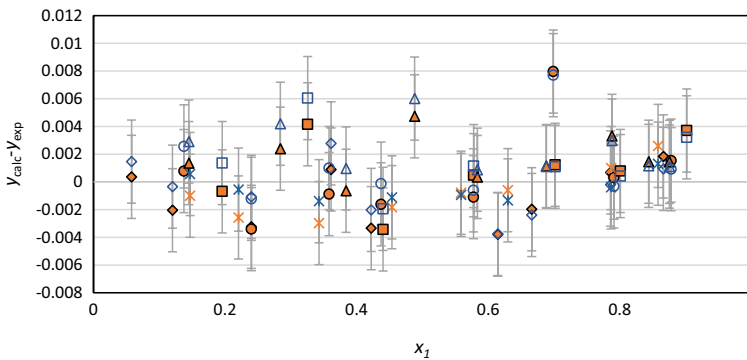


Fig. 5 Absolute deviations of vapor phase composition for the R1243zf (1)+R1243yf (2) binary mixture from PR-MC-VdW and Helmholtz models. x : 283.15 K (PR-MC-VdW model); x : 283.15 K (Helmholtz model); \diamond : 293.15 K; \circ : 303.15 K; \square : 313.15 K; Δ : 323.15 K. Solid points: PR-MC-VdW model; empty points: Helmholtz model

The thermodynamic consistency of the isothermal experimental data was verified by applying the point-to-point test method proposed by Van Ness et al. [39]. The test is based on the average absolute deviation of vapor phase mole fraction (AAD(y)), which must be less than 0.01 [12]. Since, as shown in Fig. 5, values of Δy are always lower than 0.01, the AAD(y) is necessarily lower than the threshold value, even considering the vapor phase composition uncertainties, and thus the thermodynamic consistency for the experimental values can be considered satisfied.

Figure 6 shows the relative volatilities obtained with the two models compared with the experimental ones, which are represented by the solid red curve. The relative volatility is calculated as in Eq. 14

Table 6 Calculation deviations of PR-MC-VdW and Helmholtz models

	PR-MC-vdW	Helmholtz
AAD ($\Delta p\%$) ^a	0.409	0.192
Bias ($\Delta p\%$) ^b	- 0.399	0.183
AAD (Δy) ^c	0.002	0.002
Bias (Δy) ^d	0.0002	0.0008

$$^a AAD(\Delta p\%) = \frac{100}{N_p} \sum_{i=1}^{N_p} \left(\frac{|\Delta p|}{p_{exp}} \right)_i$$

$$^b Bias(\Delta p\%) = \frac{100}{N_p} \sum_{i=1}^{N_p} \left(\frac{\Delta p}{p_{exp}} \right)_i$$

$$^c AAD(\Delta y) = \frac{1}{N_p} \sum_{i=1}^{N_p} (|\Delta y|)_i$$

$$^d Bias(\Delta y) = \frac{1}{N_p} \sum_{i=1}^{N_p} (\Delta y)_i$$

$$\alpha_{1,2} = \frac{k_1}{k_2} = \frac{y_1 \cdot x_2}{y_2 \cdot x_1} \tag{14}$$

where the subscripts 1 and 2 refer to R1243zf and R1234yf, respectively. As it can be seen, both the Helmholtz model and the PR-MC-VdW model are in good agreement with the experimental volatilities, with deviations always within 5 % from the red curve (except for one outlier). Moreover, in Fig. 6, data are further compared with predicted values calculated using the Helmholtz-type EoS implemented in REFPROP 10.0. Since no thermodynamic data for this binary mixture have been published but the one from Yang et al. [27], in this software no dedicated parameters of the Helmholtz EoS are adopted for the R1243zf/R1234yf system; instead, the binary interaction parameters for the mixture R1234yf/R1234zeE are used and a mismatch from the experimental relative volatilities is evident, thus underlining the

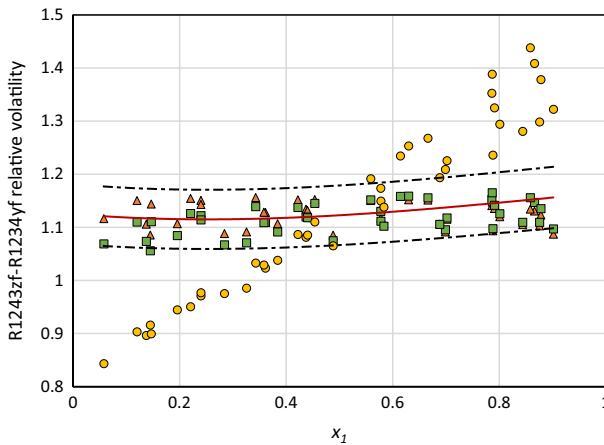


Fig. 6 Relative volatilities of the R1243zf (1)+R1234yf (2) binary mixture. ●: values from the REFPROP 10.0 software; Δ: PR-MC-VdW EoS as in Eq. 1; □: Helmholtz EoS as in Eq. 9; Solid line: experimental values from this work; dashed lines show ± 5 % from experimental data

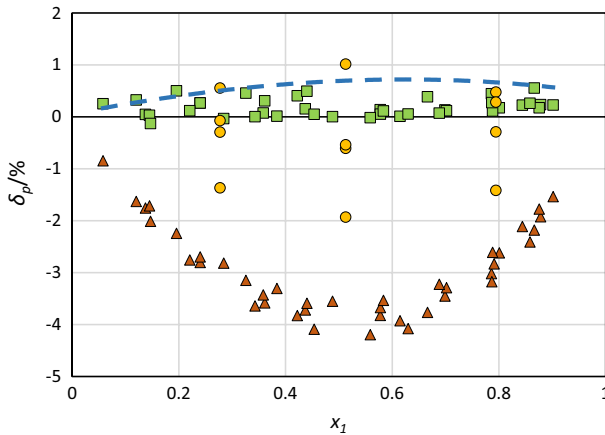


Fig. 7 Relative deviations of pressure between experimental and calculated data from this work and predictions of the REFPROP 10.0 software for the R1243zf (1)+R1234yf (2) binary mixture. ●: experimental data by Yang et al. [27]; □: experimental data from this work; dashed line: pressure values from the PR-MC-VdW EoS as in Eq. 1; Δ: pressure values from the REFPROP 10.0 software. The baseline represents calculated values from the Helmholtz EoS as in Eq. 9

fact that the Helmholtz EoS may not be effective when dedicated parameters are not regressed, unlike in the present work.

Finally, to further evaluate the consistency of the experimental data and to quantify the error committed by applying the BIPs implemented in REFPROP Fig. 7 shows the relative deviations of pressure between values measured in this work, the 12 bubble points measured by Yang et al. [27] and the REFPROP 10.0 predictions, where the baseline represents the Helmholtz EoS with dedicated binary parameters as in Eq. 9. As already shown in Fig. 4, the two models applied in this study agree well with the experimental data in terms of relative pressure, whereas the experimental data from Yang et al. [27] show scattered deviations from the Helmholtz model up to -1.93% at 333.15 K. As regards the REFPROP 10.0 model, U-shaped systematic deviations are observed, with a maximum deviation of -4.2% relative pressure.

4 Conclusion

In this study the VLE of the R1243zf/R1234yf binary mixture was isothermally measured with high reliability using a vapor recirculation apparatus at 5 temperatures from 283.15 K to 323.15 K, while in the same temperature range 10 vapour pressure data of the pure compounds were measured and compared with literature data and the Helmholtz EoS implemented in REFPROP 10.0. A modified PR EoS and a Helmholtz-type EoS were implemented to successfully reproduce the experimental VLE data. The average absolute deviation of pressure (AAD(p)) and the average absolute deviation of vapor phase mole fraction (AAD(y)) are 0.409 % and 0.002, respectively, for PR-MC -VdW model, and 0.192 % and 0.002, respectively,

for the Helmholtz model. Furthermore, predictions from the Helmholtz-type EoS currently implemented in the REFPROP 10.0 software for the binary mixture demonstrated systematic deviations of up to 4.5 % from the experimental data from this work, highlighting the importance of regressing dedicated binary interaction parameters on experimental thermophysical data.

Author Contributions GL, DM and MS performed the measurements, DM and GL performed the modeling, LF and SB revised the experimental data. All authors reviewed the manuscript.

Funding This research did not receive any specific grant from funding agencies in the public, commercial, or not-for-profit sectors.

Data Availability Not applicable.

Declarations

Competing Interests The authors have no competing interests, or other interests that might be perceived to influence the results and/or discussion reported in this paper.

Ethical Approval Not applicable.

Open Access This article is licensed under a Creative Commons Attribution 4.0 International License, which permits use, sharing, adaptation, distribution and reproduction in any medium or format, as long as you give appropriate credit to the original author(s) and the source, provide a link to the Creative Commons licence, and indicate if changes were made. The images or other third party material in this article are included in the article's Creative Commons licence, unless indicated otherwise in a credit line to the material. If material is not included in the article's Creative Commons licence and your intended use is not permitted by statutory regulation or exceeds the permitted use, you will need to obtain permission directly from the copyright holder. To view a copy of this licence, visit <http://creativecommons.org/licenses/by/4.0/>.

References

1. A. Mota-Babiloni, P. Makhnatch, Predictions of European refrigerants place on the market following F-gas Regulation restrictions. *Int. J. Refrig.* **127**, 101 (2021). <https://doi.org/10.1016/j.ijrefrig.2021.03.005>
2. “The Kigali Amendment to the Montreal Protocol: HFC Phase-down.” United Nations Environment Programme (2016). <https://wedocs.unep.org/20.500.11822/26589>
3. European Parliament and Council of the European Union. Regulation (EU) No 517/2014 of the European Parliament and of the Council of 16 April 2014 on fluorinated greenhouse gases and repealing Regulation (EC) No 842/2006 Text with EEA relevance” (2014). <http://data.europa.eu/eli/reg/2014/517/oj>
4. IPCC: Climate Change 2021, The Physical Science Basis: the Working Group I contribution to the Sixth Assessment Report of the Intergovernmental Panel on Climate Change (IPCC) (2021)
5. S. Bobbo, G. Di Nicola, C. Zilio, J.S. Brown, L. Fedele, Low GWP halocarbon refrigerants: a review of thermophysical properties. *Int. J. Refrig.* **90**, 181–201 (2018). <https://doi.org/10.1016/j.ijrefrig.2018.03.027>
6. B.K. Sovacool, S. Griffiths, J. Kim, M. Bazilian, Climate change and industrial F-gases: a critical and systematic review of developments, sociotechnical systems and policy options for reducing synthetic greenhouse gas emissions. *Renew. Sustain. Energy Rev.* **141**, 110759 (2021). <https://doi.org/10.1016/j.rser.2021.110759>
7. I. Bell, D. Riccardi, A. Bazyleva, M. McLinden, Survey of data and models for refrigerant mixtures containing halogenated olefins. *J Chem Eng Data* (2021). <https://doi.org/10.1021/acs.jced.1c00192>

8. S. Peng, S. Li, Z. Yang, Y. Duan, Vapor-liquid equilibrium measurements for the binary mixtures of pentafluoroethane (R125) with 2,3,3,3-Tetrafluoroprop-1-ene (R1234yf) and 3,3,3-Trifluoropropene (R1243zf). *Int. J. Refrig.* **134**, 115–125 (2022). <https://doi.org/10.1016/j.ijrefrig.2021.11.023>
9. Z. Yang, A. Valtz, C. Coquelet, J. Wu, J. Lu, Experimental measurement and modelling of vapor-liquid equilibrium for 3,3,3-trifluoropropene (R1243zf) and trans-1,3,3,3-tetrafluoropropene (R1234ze(E)) binary system. *Int. J. Refrig.* **120**, 137–149 (2020). <https://doi.org/10.1016/j.ijrefrig.2020.08.016>
10. Z. Yang et al., Analysis of lower GWP and flammable alternative refrigerants. *Int. J. Refrig.* **126**, 12–22 (2021). <https://doi.org/10.1016/j.ijrefrig.2021.01.022>
11. L. Fedele, S. Bobbo, D. Menegazzo, An update on the thermophysical properties data available for pure low GWP refrigerants (2021). <https://doi.org/10.18462/iir.TPTPR.2021.1985>
12. X. Yao et al., Experimental measurement of vapor-liquid equilibrium for 3,3,3-trifluoropropene(R1243zf) + 1,1,1,2-tetrafluoroethane(R134a) at temperatures from 243.150 to 293.150 K. *Int. J. Refrig.* **120**, 97–103 (2020). <https://doi.org/10.1016/j.ijrefrig.2020.09.008>
13. Y. Higashi, N. Sakoda, Measurements of PvT properties, saturated densities, and critical parameters for 3,3,3-trifluoropropene (HFO1243zf). *J. Chem. Eng. Data* **63**, 3818–3822 (2018). <https://doi.org/10.1021/acs.jced.8b00452>
14. Y. Higashi, N. Sakoda, M.A. Islam, Y. Takata, S. Koyama, R. Akasaka, Measurements of saturation pressures for trifluoroethene (R1123) and 3,3,3-trifluoropropene (R1243zf). *J. Chem. Eng. Data* **63**, 417–421 (2018). <https://doi.org/10.1021/acs.jced.7b00818>
15. Z. Yang, X. Tang, J. Wu, J. Lu, Experimental measurements of saturated vapor pressure and isothermal vapor-liquid equilibria for 1,1,1,2-tetrafluoroethane (HFC-134a) + 3,3,3-trifluoropropene (HFO-1243zf) binary system. *Fluid Phase Equilib.* **498**, 86–93 (2019). <https://doi.org/10.1016/j.fluid.2019.06.020>
16. J. Yin, J. Ke, G. Zhao, S. Ma, Saturated vapor pressure and gaseous pvT property measurements for 3,3,3-trifluoroprop-1-ene (R1243zf). *Int. J. Refrig.* **117**, 175–180 (2020). <https://doi.org/10.1016/j.ijrefrig.2020.04.021>
17. J. Brown, G. Nicola, L. Fedele, S. Bobbo, C. Zilio, Saturated pressure measurements of 3,3,3-trifluoroprop-1-ene (R1243zf) for reduced temperatures ranging from 0.62 to 0.98. *Fluid Phase Equilib.* **351**, 48–52 (2013). <https://doi.org/10.1016/j.fluid.2012.09.036>
18. G. Di Nicola, J. Steven Brown, L. Fedele, M. Securo, S. Bobbo, C. Zilio, Subcooled liquid density measurements and PvT measurements in the vapor phase for 3,3,3-trifluoroprop-1-ene (R1243zf). *Int. J. Refrig.* **36**, 2209–2215 (2013). <https://doi.org/10.1016/j.ijrefrig.2013.08.004>
19. L. Ding et al., Measurements of isochoric specific heat capacity for 3,3,3-trifluoroprop-1-ene (R1243zf) at temperatures from (250 to 300) K and pressures up to 10 MPa. *J. Chem. Thermodyn.* **161**, 106494 (2021). <https://doi.org/10.1016/j.jct.2021.106494>
20. B. Sheng et al., The isochoric special heat capacity for 3,3,3-trifluoroprop-1-ene (R1243zf) at temperatures from (299 to 351) K and pressures up to 11 MPa. *J. Chem. Thermodyn.* **153**, 106319 (2021). <https://doi.org/10.1016/j.jct.2020.106319>
21. H. Chen, K. Zhang, Z. Yang, Y. Duan, Experimental speed of sound for 3,3,3-trifluoropropene (R-1243zf) in gaseous phase measured with cylindrical resonator. *J. Chem. Eng. Data* **66**, 2256–2263 (2021). <https://doi.org/10.1021/acs.jced.1c00098>
22. D. Kim et al., Thermal conductivity measurements and correlations of pure R1243zf and binary mixtures of R32 + R1243zf and R32 + R1234yf. *Int. J. Refrig.* **131**, 990–999 (2021). <https://doi.org/10.1016/j.ijrefrig.2021.07.019>
23. C. Kondou, R. Nagata, N. Nii, S. Koyama, Y. Higashi, Surface tension of low GWP refrigerants R1243zf, R1234ze(Z), and R1233zd(E). *Int. J. Refrig.* **53**, 80–89 (2015). <https://doi.org/10.1016/j.ijrefrig.2015.01.005>
24. G. Zhao, Z. Yuan, X. Zhang, J. Yin, S. Ma, Saturated liquid kinematic viscosity, surface tension and thermal diffusivity of two low-GWP refrigerants 3,3,3-trifluoropropene (R1243zf) and trans-1-chloro-3,3,3-trifluoro-1-propene (R1233zd(E)) by light scattering method. *Int. J. Refrig.* **127**, 194–202 (2021). <https://doi.org/10.1016/j.ijrefrig.2021.03.012>
25. H. Miyamoto, M. Nishida, T. Saito, Measurement of the vapour-liquid equilibrium properties of binary mixtures of the low-GWP refrigerants R1123 and R1234yf. *J. Chem. Thermodyn.* **158**, 106456 (2021). <https://doi.org/10.1016/j.jct.2021.106456>
26. T. Yamada, H. Miyamoto, N. Sakoda, Y. Higashi, Vapor-liquid equilibrium property measurements for R32/R1234yf binary mixtures in low R32 concentration. *Int. J. Thermophys.* (2020). <https://doi.org/10.1007/s10765-020-02752-2>

27. Z. Yang, A. Valtz, C. Coquelet, J. Wu, J. Lu, Critical properties and vapor-liquid equilibrium of two near-azeotropic mixtures containing HFOs. *Int. J. Refrig.* **138**, 133–147 (2022). <https://doi.org/10.1016/j.ijrefrig.2022.03.027>
28. S. Bobbo, R. Stryjek, N. Elvassore, A. Bertucco, A recirculation apparatus for vapor–liquid equilibrium measurements of refrigerants. Binary mixtures of R600a, R134a and R236fa. *Fluid Phase Equilib.* **150–151**, 343–352 (1998). [https://doi.org/10.1016/S0378-3812\(98\)00334-3](https://doi.org/10.1016/S0378-3812(98)00334-3)
29. E.W. Lemmon, I.H. Bell, M.L. Huber, M.O. McLinden, NIST Standard Reference Database 23: Reference Fluid Thermodynamic and Transport Properties-REFPROP, Version 10.0, National Institute of Standards and Technology (2018). <https://doi.org/10.18434/T4/1502528>.
30. R. Akasaka, E.W. Lemmon, Fundamental Equations of State for cis -1,3,3,3-Tetrafluoropropene [R-1234ze(Z)] and 3,3,3-Trifluoropropene (R-1243zf). *J. Chem. Eng. Data* **64**, 4679–4691 (2019). <https://doi.org/10.1021/acs.jced.9b00007>
31. M. Richter, M.O. mclinden, E.W. Lemmon, Thermodynamic Properties of 2,3,3,3-tetrafluoroprop-1-ene (R1234yf): vapor pressure and $p - \rho - T$ measurements and an equation of state. *J. Chem. Eng. Data* **56**, 3254–3264 (2011). <https://doi.org/10.1021/je200369m>
32. K. Tanaka, Y. Higashi, Thermodynamic properties of HFO-1234yf (2,3,3,3-tetrafluoropropene). *Int. J. Refrig.* **33**, 474–479 (2010). <https://doi.org/10.1016/j.ijrefrig.2009.10.003>
33. G. Di Nicola, F. Polonara, G. Santori, Saturated pressure measurements of 2,3,3,3-tetrafluoroprop-1-ene (HFO-1234yf). *J. Chem. Eng. Data* **55**, 201–204 (2010). <https://doi.org/10.1021/je900306v>
34. L. Fedele, S. Bobbo, F. Groppo, J.S. Brown, C. Zilio, Saturated pressure measurements of 2,3,3,3-tetrafluoroprop-1-ene (R1234yf) for reduced temperatures ranging from 0.67 to 0.93. *J. Chem. Eng. Data* **56**, 2608–2612 (2011). <https://doi.org/10.1021/je2000952>
35. R. Hulse, R. Singh, H. Pham, Physical properties of HFO-1234yf, in *Proceedings of the 3rd Conference on Thermophysical Properties and Transfer Processes of Refrigerants*, Paper 178 (2009). <https://iifir.org/en/fridoc/physical-properties-of-hfo-1234yf-26354>
36. A. Valtz, J. El Abbadi, C. Coquelet, C. Houriez, Experimental measurements and modelling of vapour-liquid equilibrium of 2,3,3,3-tetrafluoropropene (R-1234yf) + 1,1,1,2,2-pentafluoropropane (R-245cb) system. *Int. J. Refrig.* **107**, 315–325 (2019). <https://doi.org/10.1016/j.ijrefrig.2019.07.024>
37. O. Kunz, W. Wagner, The GERG-2008 wide-range equation of state for natural gases and other mixtures: an expansion of GERG-2004. *J. Chem. Eng. Data* **57**, 3032–3091 (2012). <https://doi.org/10.1021/je300655b>
38. G. Ardizzon, G. Cavazzini, G. Pavesi, Adaptive acceleration coefficients for a new search diversification strategy in particle swarm optimization algorithms. *Inf. Sci. (NY)* **299**, 337–378 (2015). <https://doi.org/10.1016/j.ins.2014.12.024>
39. H.C. Van Ness, S.M. Byer, R.E. Gibbs, Vapor-Liquid equilibrium: Part I. An appraisal of data reduction methods. *AIChE J.* **19**, 238–244 (1973). <https://doi.org/10.1002/aic.690190206>
40. I.H. Bell, E.W. Lemmon, Automatic fitting of binary interaction parameters for multi-fluid Helmholtz-energy-explicit mixture models. *J. Chem. Eng. Data* **61**, 3752–3760 (2016)

Publisher's Note Springer Nature remains neutral with regard to jurisdictional claims in published maps and institutional affiliations.

Authors and Affiliations

L. Fedele¹ · G. Lombardo^{1,2} · D. Menegazzo^{1,2} · M. Scattolini¹ · S. Bobbo¹

¹ Istituto per le Tecnologie della Costruzione, Consiglio Nazionale delle Ricerche, Corso Stati Uniti 4, 35127 Padua, Italy

² Dipartimento di Ingegneria Industriale, Università degli Studi di Padova, Via Venezia 1, 35131 Padua, Italy